JTCM Journal of Traditional Chinese Medicine

Online Submissions: http://www.journaltcm.com
ISSN 0255-2922
info@journaltcm.com

Original Article

Neferine inhibits the progression of diabetic nephropathy by modulating the miR-17-5p/nuclear factor E2-related factor 2 axis

HUANG Hongmei, YANG Maojun, LI Ting, WANG Dandan, LI Ying, TANG Xiaochi, YUAN Lu, GU Shi, XU Yong

HUANG Hongmei, YANG Maojun, LI Ting, WANG Dandan, LI Ying, TANG Xiaochi, YUAN Lu, GU Shi, Department of Endocrinology, Chengdu Shuangliu District First People's Hospital (West China Airport of Sichuan University), Chengdu 610200, China
XU Yong, Department of Endocrinology, Affiliated Hospital of Southwest Medical University, Luzhou 646000, China
Supported by the Chengdu Health and Wellness Commission: Exploring the Mechanism of Neferine on Diabetic Nephropathy Based on miR-17/Nrf2 Axis (No. 2021127)
Correspondence to: Prof. XU Yong, Department of Endocrinology, Affiliated Hospital of Southwest Medical University, Luzhou 646000, China. zzh1911@sina.com
Telephone: +86-15928418055
DOI: 10.19852/j.cnki.jtcm.20231204.004
Received: December 12, 2023
Accepted: March 17, 2023
Available online: December 4, 2023

Abstract

OBJECTIVE: To investigate the effect of Neferine (Nef) on diabetic nephropathy (DN) and to explore the mechanism of Nef in DN based on miRNA regulation theory.

METHODS: A DN mouse model was constructed and treated with Nef. Serum creatinine (Crea), blood urea (UREA) and urinary albumin were measured in mice by kits, and renal histopathological changes and fibrosis were observed by hematoxylin-eosin staining and Masson staining. Renal tissue superoxide dismutase (SOD), malondialdehyde (MDA) and glutathione peroxidase (GSH-Px) activities were measured by enzyme-linked immunosorbent assay (ELISA). Western blotting was used to detect the expression of nuclear factor E2-related factor 2 (Nrf2)/ heme oxygenase 1 (HO-1) signaling pathway-related proteins in kidney tissues. Quantitative reverse transcription-polymerase chain reaction (qRT-PCR) was used to detect the expression of miR-17-5p in kidney tissues. Subsequently, a DN in vitro model was constructed by high glucose culture of human mesangial cells (HMCs), cells were transfected with miR-17-5p mimic and/or treated with Nef, and we used qRT-PCR to detect cellular miR-17 expression, flow cytometry to detect apoptosis, ELISAs to detect cellular SOD, MDA, and GSH-Px activities, Western blots to detect Nrf2/HO-1 signaling pathway-related protein expression, and dual luciferase reporter gene assays to verify the targeting relationship between Nrf2 and miR-17-5p.

RESULTS: Administration of Nef significantly reduced the levels of blood glucose, Crea, and UREA and the expression of miR-17-5p, improved renal histopathology and fibrosis, significantly reduced MDA levels, elevated SOD and GSH-Px activities, and activated Nrf2 expression in kidney tissues from mice with DN. Nrf2 is a post-transcriptional target of miR-17-5p. In HMCs transfected with miR-17-5p mimics, the mRNA and protein levels of Nrf2 were significantly suppressed. Furthermore, miR-17-5p overexpression and Nef intervention resulted in a significant increase in high glucose-induced apoptosis and MDA levels in HMCs and a significant decrease in the protein expression of HO-1 and Nrf2.

CONCLUSION: Collectively, these results indicate that Nef has an ameliorative effect on DN, and the mechanism may be through the miR-17-5p/Nrf2 pathway.

Keywords: diabetic nephropathies; neferine; miR-17-5p; NF-E2-related factor 2; oxidative stress

1. INTRODUCTION

Diabetic nephropathy (DN) is one of the most common chronic microvascular complications of diabetes mellitus (DM) and is a common cause of end-stage renal failure. DN affects approximately 30% of DM patients, and the incidence is increasing yearly, threatening the life and health of patients.[1] The hyperglycemic environment leads to inflammation and causes oxidative stress in patients with DM, which has become a risk factor for DN.[2] Numerous studies have shown that oxidative stress accelerates the progression of DN.[3,4] An increase in malondialdehyde (MDA) and downregulation of antioxidant enzymes such as superoxide dismutase (SOD) and glutathione (GSH) were observed in the kidneys of rats with type 2 diabetic mellitus (T2DM), and the restoration of these enzymes inhibited hyperglycemia-induced oxidative stress and maintained renal function.[2] However, no treatment has been identified that can cure DN.

Neferine (Nef) is a bisbenzyl isoquinoline alkaloid derived from the green germ of mature seeds of the water

lily family that has antitumor, anti-inflammatory, and antioxidant effects.[5,6] Nef was shown to have antioxidant and anti-inflammatory effects on carbon tetrachloride-induced liver fibrosis through inhibition of the mitogen-activated protein kinase and nuclear factor-κB/inhibitor of nuclear factor κB subunit α pathways.[7] In addition, Nef could inhibit high glucose-induced oxidative stress injury in rat proximal renal tubular epithelial cells by reducing reactive oxygen species (ROS) and MDA and inducing heme oxygenase 1 (HO-1) expression.[8] Nuclear factor E2-related factor 2 (Nrf2) is an important transcription factor that regulates the cellular oxidative stress response. HO-1 is one of the antioxidant proteins regulated by Nrf2, and the Nrf2/HO-1 pathway is activated in the antioxidant treatment of DN and may be an important therapeutic target for DN.[9,10] Studies have confirmed that miRNAs are closely associated with DN and play extremely important roles in DN development. For example, He *et al* [11] found that miR-320a overexpression promoted foot cell injury in mice with DN. MiR-17-5p belongs to the miR-17-92 family, and miR-17-5p mediates adipocyte differentiation and angiogenesis through the regulation of hypoxia-inducible factor 1α.[12] Our previous study identified Nrf2 as a target gene for miR-17,[13] and miR-17 was shown to be upregulated in the urine of DN patients, but the mechanism is unclear.[14] Therefore, we hypothesized that miR-17-5p is a potential executor of the antioxidant effect of Nef on DN, which affects the course of DN by targeting Nrf2 and mediating the Nrf2/HO-1 signaling pathway. To address this question, we selected C57BL/6 male mice as comparators in this study, and the glycemic changes, histopathology, oxidative stress, and miR-17-5p expression were compared in mice with DN after treatment with Nef. Furthermore, high glucose-induced human mesangial cells (HMCs) were used, and we observed the effect of Nef-mediated miR-17-5p on oxidative stress damage in HMCs to explore the mechanism of Nef in DN, which could provide an important basis for the treatment of DN.

2. MATERIALS AND METHODS

2.1. Animal experiments

Six-week-old male specific pathogen free-grade C57BL/6 mice were obtained from Chengdu Dashuo Laboratory Animal Co., Ltd. (Chengdu, China), and housed at a temperature of (25 ± 1) ℃, relative humidity of 65% ± 10%, and a 12 h light-dark cycle. All studies were conducted following the recommendations of the Guide for the Care and Use of Laboratory Animals and in compliance with the regulations of the Sichuan Provincial Laboratory Animal Management Committee, and this study was approved by the Animal Ethics Committee of West China Hospital, Sichuan University (IACUC 20220613002). Every effort was made to minimize animal suffering and reduce the number of animals used in the experiments.

2.2. Experimental design

Seven mice were randomly selected as the control group (control) and fed standard chow (Chengdu Dashuo Laboratory Animal Co., Ltd. Chengdu, China). The remaining mice were the modeling group and were fed standard chow for 7 d and given mixed chow (standard chow + high-fat chow) for 3 d, and then, high-fat chow (with 60 kcal% fat, Beijing Huafukang Biotechnology Co., Ltd., Beijing, China) was fed continuously for 1 month to induce DN. The mice were injected intraperitoneally with 100 mg/kg streptozotocin (STZ, Sigma, St. Louis, MO, USA) in citrate buffered solution (0.1 mol/L, pH 4.5) and continued to be fed a high-fat diet for 1 week, and their fasting blood glucose and urinary albumin levels were measured. The fasting blood glucose value (≥ 11.1 mmol/L) and the urinary albumin level in the model group were significantly higher than those in the control group, which indicated successful DN modeling.[15] The thirty-five successfully modeled DN mice were randomly divided into five groups of 7 mice each: the model group (DN), DN + rosiglitazone group (DN + RSG), DN + neferine low dose group (DN + Nef-L, 60 mg/kg), DN + neferine medium dose group (DN + Nef-M, 120 mg/kg), and DN + neferine high dose group (DN + Nef-H, 240 mg/kg). The mice in the DN + Nef-L, DN + Nef-M, and DN + Nef-H groups were gavaged with 60, 120, and 240 mg/kg neferine, respectively; the mice in the DN+RSG group were gavaged with 4 mg/kg RSG; and the mice in the control group and the DN group were gavaged with the same amount of saline once a day for 12 weeks. Blood was collected from the tail vein to measure the blood glucose (BG) value of the mice; urine was collected to detect the urinary albumin content, and the kidneys were weighed. The weight of the kidneys on the left and right sides (mg) was divided by the body weight of the mice (g) as the kidney weight index (mg/g). Among them, two mice in the model group died during the experiment, and we supplemented the sample size to n = 7 to have a consistent sample.

2.3. Cell culture and determination of cell proliferation

HMCs were purchased from Procell Life Science & Technology Co., Ltd. (Wuhan, China), and cultured in 1640 medium containing 10% fetal bovine serum (sugar content 5.5 mmol/L, containing 100 U/mL penicillin and 100 U/mL streptomycin, Procell Life Science and Technology, Wuhan, China) at 37 ℃ in a 5% CO_2 cell culture incubator. The effect of Nef on the proliferative activity of HMCs was detected by the cell counting kit-8 (CCK-8) method. HMCs at the logarithmic growth stage were collected and prepared into cell suspensions at a concentration of 2×10^5 cells/mL and inoculated in 96-well plates (Biolgix, Shanghai, China) at approximately 2×10^4 cells per well (100 μL), followed by the addition of Nef at final concentrations of 0.1, 0.5, 1, 2, 4, and 8 mg/mL, with complete medium but no Nef added as a control. The cells were incubated in a 5% CO_2 cell

incubator at 37 ℃ for 72 h. Ten microliters of CCK-8 solution was added to each well, and the incubation was continued for 2 h. The absorbance (A) was measured at 450 nm using an enzyme marker (SpectraMax PLUS 384, Molecular Devices LLC., San Jose, CA, USA), and the mean value of each concentration group was calculated using four replicate wells of A per group.

2.4. Mimic transfection

Experimental cells were divided into five groups: the normal control (control) group (medium with 5.5 mmol/L glucose), the high glucose group (HG) (medium with 25 mmol/L glucose), the high glucose + Nef group (HG+ Nef) (medium with 1 mg/mL of Nef and 25 mmol/L glucose), the high glucose + Nef + NC mimic group (HG + Nef + NC mimic) (medium was supplemented with 1 mg/mL of Nef and 25 mmol/L glucose and transfected with NC mimic) and the high glucose + Nef + miR-17 mimic group (HG + Nef + miR-17 mimic) (medium was supplemented with 1 mg/mL of Nef and 25 mmol/L glucose and transfected with miR-17 mimic). The transfection of NC mimic and miR-17 mimic (RiboBio, Guangzhou, China) was performed according to the Lipofectamine 2000 reagent instructions (Invitrogen, Carlsbad, CA, USA), 16 HMCs were inoculated in 6-well plates at 1×10^5 cells/well 1 d before transfection, and cells were transfected when they reached 80%-90% confluence. Cells were collected 48 h after transfection for further analysis.

2.5. Luciferase activity assay

Wild-type and mutant NFE2L2-3' untranslated region (3'UTR) were cloned into the pGL3-promoter vector. Afterward, 500 ng of pGL3-NFE2L2-WT or pGL3-NFE2L2-Mut constructs with miR-17-5p mimic or negative control (NC mimic) was transfected into 293T cells (2×10^4), and 48 h later, experiments were performed according to the dual luciferase assay instructions (Solarbio, Beijing, China) based on the firefly fluorescence intensity/sea kidney fluorescence intensity ratio to reflect the relative fluorescence intensity of different treatment groups.[17]

2.6. Cell apoptosis assay

HMCs cultured with different treatments were digested with trypsin, collected and prepared as single cell suspensions, and washed three times with prechilled PBS. The cells were then stained with 5 μL of Annexin V-APC (Sigma, St. Louis, MO, USA) and 5 μL of V-PE (Sigma, St. Louis, MO, USA) in the dark at room temperature. Subsequently, 10 μL of propidium iodide (PI, Sigma, St. Louis, MO, USA) was added and immediately analyzed by FACSCalibur flow cytometry (BD Biosciences, San Jose, CA, USA).

2.7. Biochemical analysis

Mouse 24 h urine was collected, mice were anesthetized with sodium pentobarbital (35 mg/kg) by intraperitoneal injection, blood was obtained through the abdominal aorta, centrifuged at 3000 r/min at 4 ℃, and the supernatant was taken. Serum creatinine (Crea) and blood urea (UREA) were determined according to the kit instructions (ZCIBIO Technology Co., Ltd., Shanghai, China), and urinary albumin (ALB) was determined according to the mouse albumin assay kit instructions (ZCIBIO Technology Co., Ltd., Shanghai, China). In addition, the levels of superoxide dismutase (SOD), malondialdehyde (MDA), and glutathione peroxidase (GSH-Px) in kidney tissues and cells were measured by enzyme-linked immunosorbent assays (ZCIBIO Technology Co., Ltd., Shanghai, China). All experimental operations were performed strictly according to the manufacturer's instructions, and each sample was assayed three times.

2.8. Histopathological examination

The kidney tissues were fixed with 4% paraformaldehyde, embedded in paraffin and serially sectioned at a thickness of 5 μm. The sections were stained with hematoxylin-eosin (HE),[18] imaged and observed for histopathology using a BA210Digital digital trinocular camera microscope system (Motic Instruments, Inc., Baltimore, MD, USA). Masson staining[19] was also performed on kidney tissues to observe renal fibrosis. The area of fibrous tissue (Area) within the acquired images was determined using the Image-Pro Plus 6.0 analysis system (Media Cybernetics, Inc., Rockville, MD, USA), and the percentage of area of fibrous tissue (%) = area of fibrous tissue/area of field of view (pixel area).

2.9. Quantitative reverse transcription polymerase chain reaction (qRT-PCR)

Cells and kidney tissues were lysed for total RNA extraction using TRIzol kits (Invitrogen, USA) according to the manufacturer's instructions. Total RNA from each sample was reverse transcribed into first-strand cDNA for qRT-PCR analysis.[20] Gene expression levels were quantified using TaKaRa TB Green ™ PreMix Ex Taq™ (RR820A, TaKaRa, Otsu, Japan), and β-actin or U6 was used as an internal reference gene. qRT-PCR conditions were as follows: initial denaturation at 95 ℃ for 10 min, followed by denaturation at 95 ℃ for 10 s, annealing at 60 ℃ for 10 s, and extension at 72 ℃ for 10 s for 45 cycles, with recording of cycle threshold values. The relative expression levels were analyzed using $2^{-\Delta\Delta Ct}$, and the experiment was repeated three times. Primer sequences were designed and synthesized by Sangon Biotech (Shanghai, China), primer sequences: Nrf2: Sense: 5'-TCCAGTCAGAAACCAGTGGAT-3', Antisense: 5'-GAATGTCTGCGCCAAAAGCTG-3'; A-actin: Sense: 5'-GAAGATCAAGATCATTGCTCC-3', Antisense: 5'-TACTCCTGCTTGCTGATCCA-3'; miR-17-5p: Sense: 5'-TCTAGATCCCGAGGACTG-3', Universal antisense:

Mir-X miRNA qRT-PCR TB Green® kit (No. 638314; Clontech, TaKaRa Bio, Inc. Otsu, Japan) provided; U6: Mir-X miRNA qRT-PCR TB Green® kit (no. 638314; Clontech, TaKaRa Bio, Inc. Otsu, Japan) provided.

2.10. Western blot analysis

Total cellular and kidney tissue proteins were extracted using radioimmunoprecipitation assay lysis buffer (BC3711, Solarbio, Beijing, China), and protein concentrations were detected using bicinchoninic acid (ab102536, Abcam, Cambridge, UK). Proteins were separated by 10% sodium dodecyl sulfate-polyacrylamide gel electrophoresis electrophoresis and transferred to polyvinylidene fluoride membranes, which were incubated with tris-buffered saline Tween-20 (TBST) containing 5% skim milk (Sigma, St. Louis, MO, USA) at room temperature for 2 h. The membranes were incubated overnight at 4 ℃ with the following primary antibodies (A0674, 1∶2000 rabbit anti-Nrf2; A11919, 1∶2000 rabbit anti-HO-1; A1352, 1∶2000 rabbit anti-Col Ⅰ; A3795, 1∶2000 rabbit anti-Col Ⅲ; AC026, 1:1000 rabbit polyclonal anti-β-actin; Abclonal, Wuhan, China), washed with TBST, incubated with goat-anti-rabbit IgG (H + L)-HRP (s0001, Affinity, Cincinnati, OH, USA) for 2 h at room temperature, mixed with ECL luminescent solution (Sigma, St. Louis, MO, USA) for color development and photographed in an autoexposure meter. The grayscale value of each protein band was analyzed by ImagePro Plus software (Media Cybernetics, Silver Spring, MD, USA), and the relative protein expression was calculated.[21]

2.11. Statistical analysis

Data were statistically analyzed using SPSS 22.0 statistical software (IBM Corp., Armonk, NY, USA) and are expressed as mean ± standard deviation ($\bar{x} \pm s$). Least significant difference-*t* tests were used to analyze the data with only two groups, and One-way analysis of variance was used to analyze the differences among multiple groups, with $P < 0.05$ indicating that the differences were statistically significant.

3. RESULTS

3.1. Effect of Nef on blood biochemistry and blood glucose in mice with DN

The results showed that the levels of BG, Crea, UREA, and ALB were significantly increased in the DN group, and the levels of BG, Crea, UREA, and ALB were significantly reduced in the DN + Nef-H group compared with the DN group ($P < 0.05$). Compared with those of the DN + RSG group, the levels of Crea and UREA were significantly decreased in the DN + Nef-H group ($P < 0.05$), indicating that the renal function of the mice with DN was weaker than that of the control group. However, Nef-H significantly improved the renal function of mice (Table 1).

3.2. Effect of Nef on kidney histopathology in mice with DN

To confirm the effect of Nef on the pathological morphology of mice with DN, we performed histopathological examinations of the mice. The results showed that compared with those of the control group, the renal tubercle structure was damaged, the basement membrane of the renal capsule was thickened more obviously, the epithelial cell nuclei were swollen, a small amount of fibrous tissue proliferation and a small amount of lymphocytes were scattered in the local interstitium (Figure 1A), and there was a significant increase in the percentage of positive collagen fiber area (Figure 1B, 1C) and kidney weight index (Figure 1D) in the mice with DN. However, the kidney tissue peritoneum was more intact in the DN + RSG, DN-Nef-M, and DN-Nef-H groups, no connective tissue hyperplasia or inflammatory exudation was observed, and the percentage of collagen fiber-positive area and kidney weight index were significantly reduced ($P < 0.05$), indicating that the pathological morphology of the mice with DN was significantly improved after Nef treatment.

3.3. Effect of Nef on renal oxidative stress indicators in mice with DN

To further verify the effect of Nef on oxidative stress in the mice with DN, we investigated relevant parameters by ELISAs. The present results revealed that the levels of MDA were significantly increased, and the levels of SOD and GSH-Px were significantly decreased in the kidney tissues of the mice in the DN group compared to those of the control group ($P < 0.05$). Compared with those in the DN group, the levels of MDA were markedly decreased, and the levels of SOD and GSH-Px were dramatically increased in the kidney tissues of the mice in the DN+RSG, DN-Nef-L, DN-Nef-M, and DN-Nef-H

Table 1 Blood biochemistry and blood glucose of each group of mice ($\bar{x} \pm s$)

Group	*n*	BG (mmol/L)	Crea (μmol/L)	UREA (mmol/L)	ALB (g/L)
Control	7	7.5±0.6	56.1±24.0	5.4±1.4	30.0±3.0
DN	7	22.2±0.4[a]	159.5±24.0[a]	18.6±3.2[a]	51.3±7.3[a]
DN+RSG	7	13.0±0.7[b]	99.7±13.1[b]	10.8±1.2[b]	35.6±3.9[b]
DN+Nef-L	7	17.2±0.6[b]	135.3±19.8	16.3±1.2	49.8±5.5
DN+Nef-M	7	13.9±1.1[b]	111.1±14.1[b]	11.2±2.4[b]	42.6±4.4
DN+Nef-H	7	11.5±1.1[b]	89.2±10.3[bc]	9.1±1.4[bc]	33.5±3.6[b]

Notes: DN: diabetic nephropathy; RSG: rosiglitazone (4 mg/kg); Nef-L: neferine low dose (60 mg/kg); Nef-M: neferine medium dose (120 mg/kg); Nef-H: neferine high dose (240 mg/kg). [a]$P < 0.05$, compared with the control group, [b]$P < 0.05$, compared with the DN group, [c]$P < 0.05$, compared with the DN + RSG group.

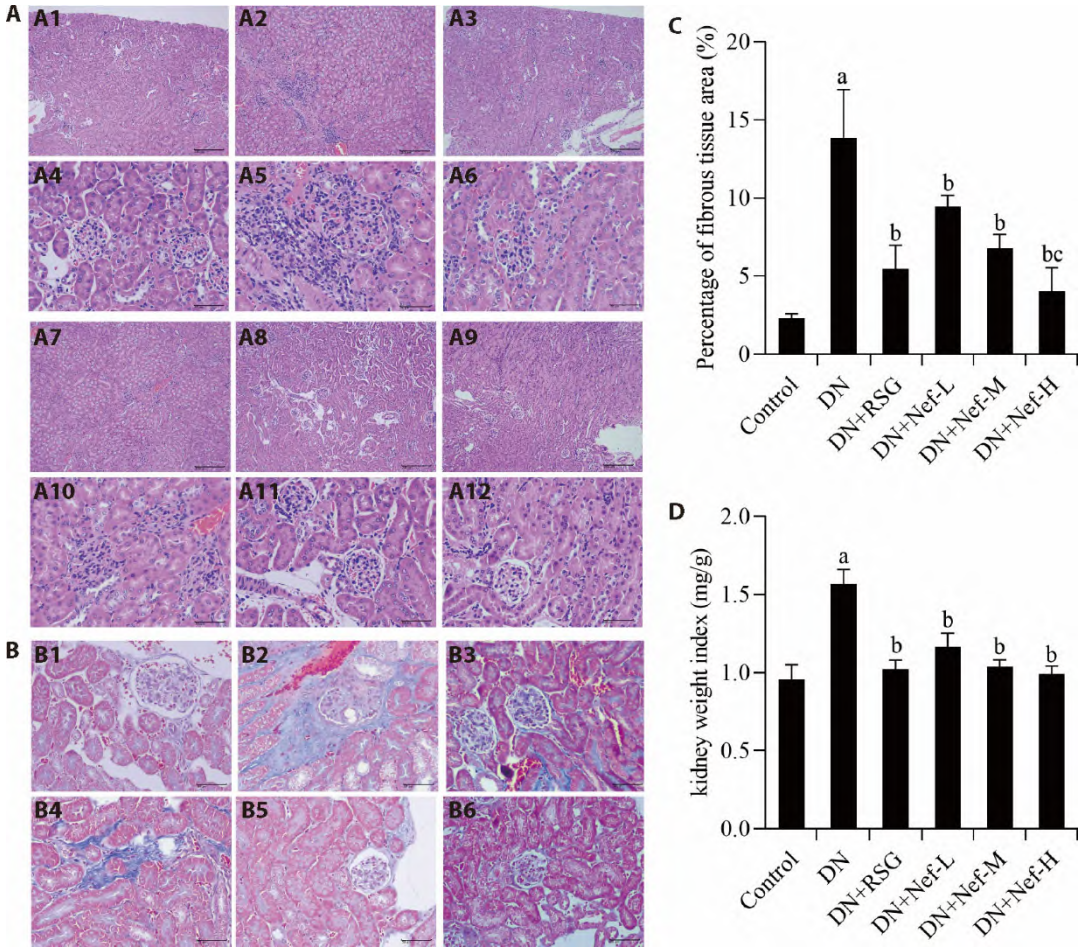

Figure 1 Effect of Nef on the kidney histopathology in mice with DN

A: HE staining of kidney tissue (scale bar, 200 μm and 50 μm); A1: control group (×100); A2: DN group (×100); A3: DN + RSG group (×100); A4: control group (×400); A5: DN group (×400); A6: DN + RSG group (×400); A7: DN-Nef-L group (×100); A8: DN-Nef-M group (×100); A9: DN-Nef-H group (×100); A10: DN-Nef-L group (×400); A11: DN-Nef-M group (×400); A12: DN-Nef-H group (×400). B: Masson staining of kidney tissue (×400, scale bar, 50 μm); B1: control group; B2: DN group; B3: DN + RSG group; B4: DN-Nef-L group; B5: DN-Nef-M group; B6: DN-Nef-H group. C: percentage of positive collagen fiber area (%); D: kidney weight index of the mice. DN: diabetic nephropathy; HE: hematoxylin and eosin; RSG: rosiglitazone (4 mg/kg); Nef-L: neferine low dose (60 mg/kg); Nef-M: neferine medium dose (120 mg/kg); Nef-H: neferine high dose (240 mg/kg). Data were statistically analyzed by least significant difference. Data were expressed as mean ± standard deviation (n =3). $^{a}P < 0.05$, compared with the control group; $^{b}P < 0.05$, compared with the DN group; $^{c}P < 0.05$, compared with the DN + RSG group.

groups ($P < 0.05$). Compared with those in the DN+RSG group, the levels of GSH-Px were significantly increased in the kidney tissues of the mice in the DN-Nef-H group ($P < 0.05$, Figure 2A). Moreover, the protein expression of HO-1, Nrf2, Col Ⅰ, and Col Ⅲ in the mouse kidney tissues was detected using Western blotting, and the results showed that the protein expression of Col Ⅰ and Col III was significantly increased, while the protein expression of HO-1 and Nrf2 was significantly decreased in the DN group ($P < 0.05$). Nef-H significantly reversed the protein expression of Nrf2, Col Ⅰ, and Col Ⅲ in the mice with DN (Figure 2B). Nef-H attenuated oxidative stress damage caused by DN.

3.4. Targeting relationship between Nrf2 and miR-17-5p and the effect of Nef on renal miR-17-5p expression in the mice with DN

Screening by the target gene prediction database (http://www.targetscan.org) revealed that the Nrf2 gene binding site is complementary to miR-17-5p and may be a target gene downstream of miR-17-5p. After the gene reporter plasmid of wild-type Nrf2 3′-UTR was cloned and cotransfected with miR-17-5p mimic, the luciferase activity was significantly attenuated, while cotransfecting the gene reporter plasmid of mutant Nrf2 3′-UTR with miR-17-5p mimic did not significantly affect the luciferase activity (Figure 3A). This finding demonstrates that miR-17-5p can directly interact with the 3′ UTR of Nrf2 mRNA.

To determine the effect of Nef on miR-17-5p expression in the kidneys of the mice with DN, we detected miR-17-5p expression in mouse kidney tissue by RT–qPCR. The results showed that miR-17-5p expression was significantly increased in the kidney tissue of the mice in the DN group compared to the control group ($P < 0.05$). Compared with that of the DN group, the expression of miR-17-5p was markedly decreased in the kidney tissues of the mice in the DN-Nef-L and DN-Nef-H groups ($P < 0.05$, Figure 3B). To confirm the effect of miR-17-5p on

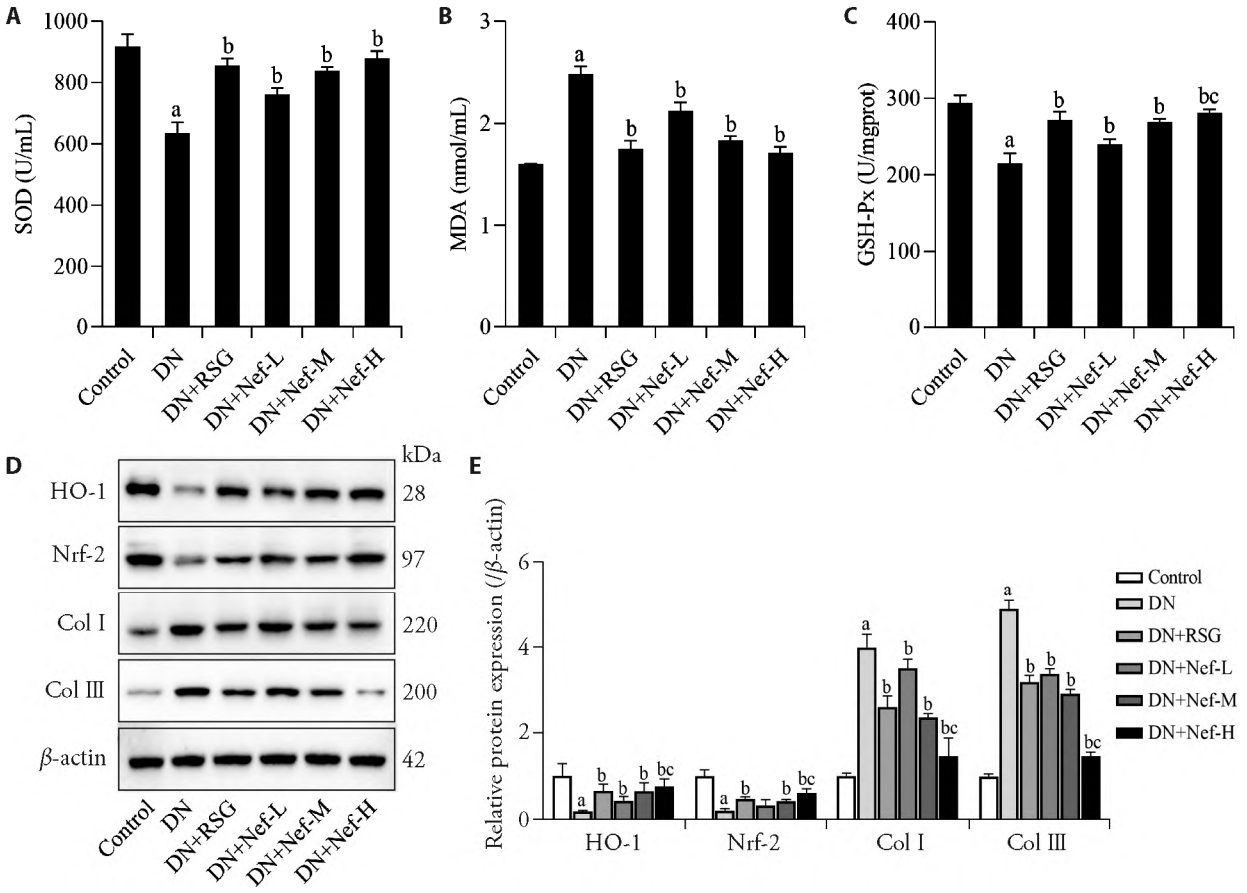

Figure 2 Effect of Nef on renal oxidative stress indicators in mice with DN

A: levels of SOD in the kidney tissues of mice. B: levels of MDA in the kidney tissues of mice. C: levels of GSH-Px in the kidney tissues of mice. D: representative blot images of HO-1, Nrf2, Col I, and Col III measured by western blot. E: protein expression of HO-1, Nrf2, Col I, and Col III in the kidney tissues of mice was detected by Western blotting. DN: diabetic nephropathy; RSG: rosiglitazone (4 mg/kg); Nef-L: neferine low dose (60 mg/kg); Nef-M: neferine medium dose (120 mg/kg); Nef-H: neferine high dose (240 mg/kg); SOD: superoxide dismutase; MDA: malondialdehyde; GSH-Px: glutathione peroxidase; HO-1: heme oxygenase 1; Nrf2: nuclear factor E2-related factor 2; Col I: collagen I; Col III: collagen III. Data were statistically analyzed by least significant difference-*t*. Data were expressed as mean ± standard deviation (n = 3). $^{a}P < 0.05$, compared with the control group, $^{b}P < 0.05$, compared with the DN group, $^{c}P < 0.05$, compared with the DN + RSG group.

Nrf2 expression, we transfected the miR-17-5p mimic or control mimic into HMCs. The results showed that miR-17-5p expression levels in HMCs were significantly enhanced after transfection with miR-17-5p mimic ($P < 0.05$), and Nrf2 mRNA levels in HMCs were significantly decreased after transfection with miR-17-5p mimic ($P < 0.05$, Figure 3B). Similarly, Nrf2 protein levels in HMCs were significantly inhibited upon transfection with miR-17-5p mimic ($P < 0.05$, Figure 3C), suggesting that Nef inhibits miR-17-5p expression, and transfection of miR-17-5p mimics inhibited Nrf2 expression in HMCs. In addition, we examined the effect of different concentrations of Nef on the proliferation of HMCs. The results showed that 2, 4, and 8 mg/mL Nef could significantly slow the proliferation of HMCs, while 0.5 and 1 mg/mL Nef had no significant effect on the proliferation of HMCs (Figure 3D). Therefore, we chose 1 mg/mL Nef for the follow-up experiments.

3.5. Effect of Nef-mediated miR-17-5p on oxidative stress injury in high glucose-induced HMCs

Next, we analyzed the effect of Nef-mediated miR-17-5p on oxidative stress injury in high glucose-induced HMCs. Compared with that of the control group, the mRNA expression of miR-17-5p was significantly increased in HMCs in the HG group ($P < 0.05$). Compared with that of the HG group, the mRNA expression of miR-17-5p in HMCs in the HG + Nef and HG + Nef + NC mimic groups was significantly decreased ($P < 0.05$); compared with that of the HG + Nef group, the mRNA expression of miR-17-5p was significantly increased in the HG + Nef + miR-17-5p mimic group ($P < 0.05$, Figure 4A). Furthermore, compared with those of the control group, the protein expression of Col Ⅰ and Col Ⅲ (Figure 4B), cell apoptosis (Figure 4C, 4D), and the level of MDA (Figure 4E) were significantly increased, while the protein expression of HO-1 and Nrf2 (Figure 4B) and the levels of SOD and GSH-Px (Figure 4E) were significantly decreased in the HG group ($P < 0.05$); compared with those of the HG group, the protein expression of Col Ⅰ and Col Ⅲ (Figure 4B), cell apoptosis (Figure 4C, D), and the level of MDA (Figure 4E) were significantly decreased, while the protein expression of HO-1 and Nrf2 (Figure 4B) and the levels of SOD and GSH-Px (Figure 4E) were significantly

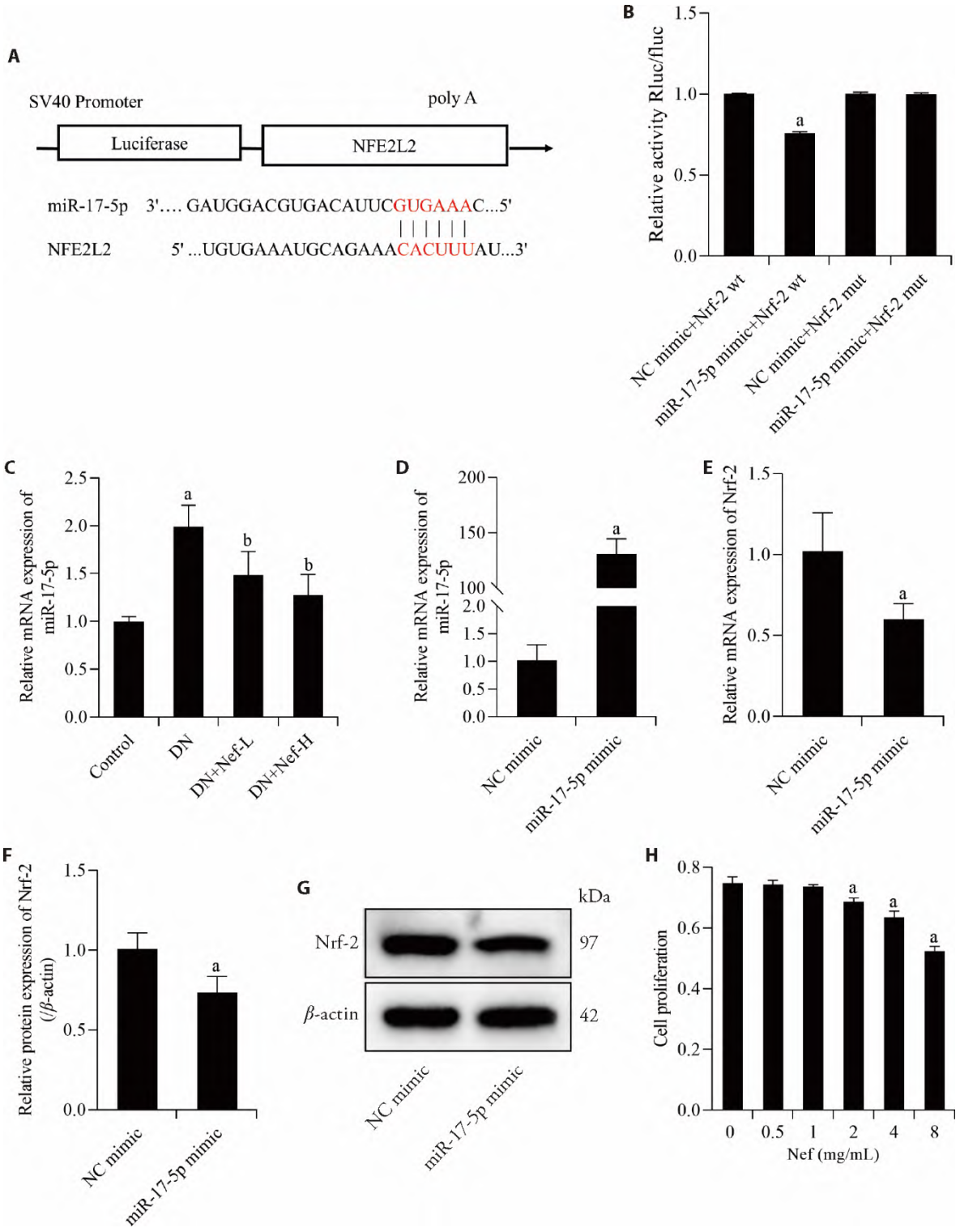

Figure 3 Targeting relationship between Nrf2 and miR-17-5p and the effect of Nef on renal miR-17-5p expression in the mice with DN
A: TargetScan (http://www.targetscan.org) prediction showing potential miR-17-5p binding sites for the Nrf2 3'-UTR, complementary pairing of target genes is indicated in red. B: miR-17-5p target sequences were fused with a luciferase reporter and transfected with miR-17-5p mimic or NC mimic into HEK-293T cells, and miR-17-5p significantly restrained the luciferase activity of the Nrf2 3'-UTR. C: mRNA level of miR-17-5p in the kidney tissues of mice. D: mRNA levels of miR-17-5p in HMCs. E: mRNA levels of Nrf2 in HMCs. F: protein expression of Nrf2 in HMCs. G: representative blot images of Nrf2. H: detection of the proliferation of HMCs treated with different concentrations of Nef. The data in qRT-PCR analysis were expressed after normalization to U6 or β-actin, while those in Western blot assays were expressed after normalization to β-actin. DN: diabetic nephropathy; Nef-L: neferine low dose (60 mg/kg); Nef-H: neferine high dose (240 mg/kg). Nrf2: nuclear factor E2-related factor 2. NC: negative control; HMCs: human mesangial cells; qRT-PCR: quantitative reverse transcription-polymerase chain reaction. Data were statistically analyzed by least significant difference-*t*. Data were expressed as mean ± standard deviation (n = 3). $^{a}P < 0.05$, compared with the control or NC mimic group; $^{b}P < 0.05$, compared with the DN group.

increased in the HG + Nef and HG + Nef + NC mimic groups ($P < 0.05$); compared with those of the HG + Nef group, the protein expression of Col I and Col III (Figure 4B), cell apoptosis (Figure 4C, 4D), and the level of MDA (Figure 4E) were significantly increased, while the protein expression of HO-1 and Nrf2 (Figure 4B) and the level of GSH-Px (Figure 4E) were significantly decreased in the HG + Nef + miR-17-5p mimic group ($P < 0.05$), showing that miR-17-5p mimic reverses the effect of Nef on oxidative stress and apoptosis in HMCs.

4. DISCUSSION

In the present study, we demonstrated that Nef ameliorated DN-induced renal lesions, attenuated oxidative stress injury induced by DN, and inhibited the expression of miR-17-5p in DN, which directly targets Nrf2. Further results showed that Nef significantly attenuated oxidative stress injury and apoptosis in human mesangial cells induced by high glucose, and transfection of the miR-17-5p mimic reversed this effect.

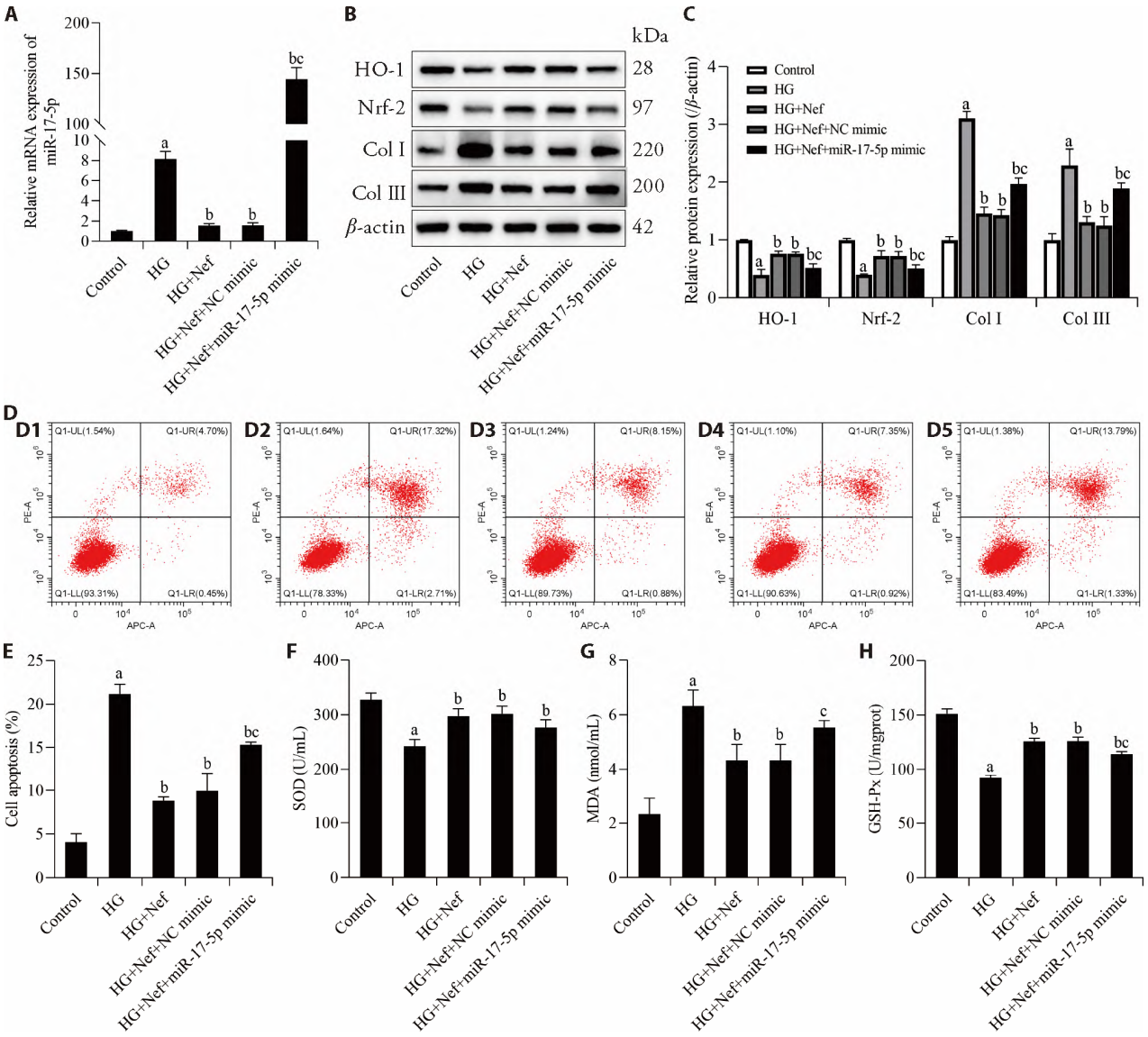

Figure 4 Effect of Nef-mediated miR-17-5p on oxidative stress injury in high glucose-induced HMCs

A: mRNA level of miR-17-5p in HMCs; B: representative blot images of HO-1, Nrf2, Col Ⅰ, and Col Ⅲ; C: protein expression of HO-1, Nrf2, Col Ⅰ, and Col Ⅲ in HMCs; D: detection of cell apoptosis using flow cytometry; D1: control group; D2: HG group; D3: HG + Nef group; D4: HG + Nef + NC mimic group; D5: HG + Nef + miR-17-5p mimic group; E: cell apoptosis; F: levels of SOD in HMCs; G: levels of MDA in HMCs; H: levels of GSH-Px in HMCs. HG: high glucose (25 mmol/L). HG + Nef: high glucose (25 mmol/L) + Nef (1 mg/mL). HG+Nef+NC mimic: high glucose (25 mmol/L) + Nef (1 mg/mL) + NC mimic. HG + Nef + miR-17-5p mimic: high glucose (25 mmol/L) + Nef (1 mg/mL) + miR-17-5p mimic. The data from the qRT-PCR analysis were normalized with U6, while those from Western blot assays were normalized with β-actin. HG: high glucose; Nef: neferine; HO-1: heme oxygenase 1; Nrf2: nuclear factor E2-related factor 2; Col Ⅰ: collagen Ⅰ; Col Ⅲ: collagen Ⅲ; SOD: superoxide dismutase; MDA: malondialdehyde; GSH-Px: glutathione peroxidase; HMCs: human mesangial cells; NC: negative control; qRT-PCR: quantitative reverse transcription-polymerase chain reaction. Data were statistically analyzed by least significant difference-*t*. Data were expressed as mean ± standard deviation ($n = 3$). [a]$P < 0.05$, compared with the control group; [b]$P < 0.05$, compared with the HG group; [c]$P < 0.05$, compared with the HG + Nef group.

Thus, the improvement of DN by Nef may be achieved through the miR-17-5p/Nrf2 pathway.

Relevant literature shows that renal-related complications gradually worsen with increased blood glucose during the development of DN.[22] The results of this study showed that compared with those of the control group, the BG, ALB, and renal function-related indices (Crea and UREA) were significantly increased in the DN group of mice, and Nef could control the level of BG in the mice with DN to a certain extent and could significantly reduce the levels of ALB, Crea, and UREA. We found that high doses of Nef had a stronger ability to reduce BG, ALB, Crea, and UREA, indicating that Nef had positive effects on renal function in DN. The early pathological changes of DN are mainly glomerular hypertrophy, and with the progression of the disease, renal body structure and thickening of the basement membrane of the renal capsule can be observed.[23] Col Ⅰ and Col Ⅲ are two collagen proteins, and studies have shown that reducing the accumulation of Col Ⅰ and Col Ⅲ delays the development of interstitial fibrosis.[24] Therefore, the present study further applied HE staining to observe the morphological changes in the kidneys in each group of mice, and the results showed that the mice in the DN group had swollen epithelial cell nuclei, narrowed renal capsule lumen, and thickened intravascular glomerular tract and basement membrane. After Nef treatment, all the above pathological changes were reduced to some extent, and the improvement was more obvious in the Nef high-dose group, which further confirmed the renoprotective effect of Nef. In addition, we performed Masson staining to observe fibrosis in the kidney and found that fibrosis was significantly increased in the DN group compared with the control group and improved significantly after Nef intervention. The results of Western blot analysis showed that the protein expression of Col Ⅰ and Col Ⅲ was significantly reduced after Nef intervention. Oxidative stress plays an extremely important role in inducing the occurrence and development of DN.[25] Studies have shown that in a high glucose state, disorders of glucose metabolism can cause a large number of oxygen radicals to be generated and oxidized with lipids to form MDA, which induces the progression of DN.[26] Nrf2 is a core transcription factor that regulates redox homeostasis in organisms. Nrf2 translocates to the nucleus to regulate transcription, which can activate the transcription of many antioxidant genes and phase Ⅱ enzyme genes, including HO-1, SOD, GSH, etc., to improve the antioxidant stress capacity of cells.[27] Moreover, GSH-Px, as a downstream antioxidant enzyme of the Nrf2 pathway, can resist oxidative stress and reduce renal damage after activation.[28] In this study, we found that compared with those of the control group, the MDA levels were significantly increased and SOD and GSH-Px activity and Nrf2 and HO-1 protein expression were significantly decreased in the mice with DN, indicating that in the DN state, there is significant oxidative stress damage in the body and the ability to resist oxidative stress is also decreased. Nef activated the protein expression of Nrf2 and HO-1, increased SOD and GSH-Px activity and decreased MDA levels, suggesting that Nef improved oxidative stress damage in DN. In addition, microRNAs (miRNAs) are noncoding endogenous small molecule RNAs 21 to 25 nucleotides in length that can regulate gene expression through post-transcriptional mechanisms.[29] Studies have confirmed that miR-17 is upregulated in the urine of DN patients.[30] Our previous study identified Nrf2 as a target gene for miR-17,[13] and Nrf2 regulates HO-1.[31] Through analysis, we found that Nrf2 was the target gene of miR-17-5p, and Nef significantly attenuated high glucose-induced oxidative stress damage and apoptosis in human mesangial cells, while elevated miR-17-5p reversed the activation of Nrf-2 and HO-1 expression by Nef, exacerbated oxidative stress and cell apoptosis, and promoted the pathological process of DN. This finding suggests that the amelioration of DN by Nef may be achieved by regulating the miR-17-5p/Nrf2 pathway.

In conclusion, the results from our study indicated that Nef can attenuate oxidative stress injury, inhibit miR-17-5p expression, promote Nrf-2 and HO-1 expression, and ultimately achieve therapeutic effects for DN. We hope our results provide a theoretical basis for the clinical development of therapeutic agents targeting miR-17-5p for the treatment of DN.

5. REFERENCES

1. Samsu N. Diabetic nephropathy: challenges in pathogenesis, diagnosis, and treatment. Biomed Res Int 2021; 2021: 1497449.
2. Dai X, Liao R, Liu C, et al. Epigenetic regulation of TXNIP-mediated oxidative stress and NLRP3 inflammasome activation contributes to SAHH inhibition-aggravated diabetic nephropathy. Redox Biol 2021; 45: 102033.
3. Gerardo Yanowsky-Escatell F, Andrade-Sierra J, Pazarín-Villaseñor L, et al. The role of dietary antioxidants on oxidative stress in diabetic nephropathy. Iran J Kidney Dis 2020; 14: 81-94.
4. Sagoo MK, Gnudi L. Diabetic nephropathy: is there a role for oxidative stress? Free Radic Biol Med 2018; 116: 50-63.
5. Tang YS, Zhao YH, Zhong Y, et al. Neferine inhibits LPS-ATP-induced endothelial cell pyroptosis *via* regulation of ROS/NLRP3/Caspase-1 signaling pathway. Inflamm Res 2019; 68: 727-38.
6. Bharathi Priya L, Huang CY. An updated review on pharmacological properties of neferine-A bisbenzylisoquinoline alkaloid from Nelumbo nucifera. J Food Biochem 2021; 45: e13986.
7. Wang Y, Wang S, Wang R, et al. Neferine exerts antioxidant and anti-inflammatory effects on carbon tetrachloride-induced liver fibrosis by inhibiting the MAPK and NF-κB/IκBα pathways. Evid Based Complement Alternat Med 2021; 2021: 4136019.
8. Li S, Zhang Y, Zhang J, et al. Neferine exerts ferroptosis-inducing effect and antitumor effect on thyroid cancer through Nrf2/HO-1/NQO1 inhibition. J Oncol 2022; 2022: 7933775.
9. Liu Y, Wang J, Zhang X, Wang L, Hao T, Cheng Y. Scutellarin exerts hypoglycemic and renal protective effects in db/db mice *via* the Nrf2/HO-1 signaling pathway. Oxid Med Cell Longev 2019; 2019: 1354345.
10. Xing L, Guo H, Meng S, et al. Klotho ameliorates diabetic nephropathy by activating Nrf2 signaling pathway in podocytes. Biochem Biophys Res Commun 2021; 534: 450-56.
11. He M, Wang J, Yin Z, et al. MiR-320a induces diabetic nephropathy *via* inhibiting MafB. Aging (Albany NY) 2019; 11: 3055-79.

12. Guo Y, Du F, Tan YL, Luo J, Xiong D, Song WT. VEGF-mediated angiogenesis in retinopathy of prematurity is co-regulated by miR-17-5p and miR-20a-5p. Biochem Cell Biol 2021; 99: 414-23.
13. Wei J, Hao Q, Chen C, et al. Epigenetic repression of miR-17 contributed to di (2-ethylhexyl) phthalate-triggered insulin resistance by targeting Keap1-Nrf2/miR-200a axis in skeletal muscle. Theranostics 2020; 10: 9230-48.
14. Du KY, Qadir J, Yang BB, Yee AJ, Yang W. Tracking miR-17-5p levels following expression of seven reported target mRNAs. Cancers (Basel) 2022; 14: 2585.
15. Cai TT, Ye XL, Li RR, et al. Resveratrol modulates the gut microbiota and inflammation to protect against diabetic nephropathy in mice. Front Pharmacol 2020; 11: 1249.
16. Wu F, Ji A, Zhang Z, Li J, Li P. miR-491-5p inhibits the proliferation and migration of A549 cells by FOXP4. Exp Ther Med 2021; 21: 622.
17. Duan YR, Chen BP, Chen F, et al. LncRNA lnc-ISG20 promotes renal fibrosis in diabetic nephropathy by inducing AKT phosphorylation through miR-486-5p/NFAT5. J Cell Mol Med 2021; 25: 4922-37.
18. Shen Y, Chen W, Han L, et al. VEGF-B antibody and interleukin-22 fusion protein ameliorates diabetic nephropathy through inhibiting lipid accumulation and inflammatory responses. Acta Pharm Sin B 2021; 11: 127-42.
19. Lee SY, An HJ, Kim JM, et al. PINK1 deficiency impairs osteoblast differentiation through aberrant mitochondrial homeostasis. Stem Cell Res Ther 2021; 12: 589.
20. Ma H, Bell KN, Loker RN. qPCR and qRT-PCR analysis: Regulatory points to consider when conducting biodistribution and vector shedding studies. Mol Ther Methods Clin Dev2021; 20: 152-68.
21. Pillai-Kastoori L, Schutz-Geschwender AR, Harford JA. A systematic approach to quantitative Western blot analysis. Anal Biochem 2020; 593: 113608.
22. Xian Y, Gao Y, Lü W, et al. Resveratrol prevents diabetic nephropathy by reducing chronic inflammation and improving the blood glucose memory effect in non-obese diabetic mice. Naunyn Schmiedebergs Arch Pharmacol 2020; 393: 2009-17.
23. Zheng C, Huang L, Luo W, et al. Inhibition of STAT3 in tubular epithelial cells prevents kidney fibrosis and nephropathy in STZ-induced diabetic mice. Cell Death Dis 2019; 10: 848.
24. Bai L, Li A, Gong C, Ning X, Wang Z. Protective effect of rutin against bleomycin induced lung fibrosis: involvement of TGF-β1/α-SMA/Col Ⅰ and Ⅲ pathway. Biofactors 2020; 46: 637-44.
25. Huang W, Man Y. Short-chain fatty acids ameliorate diabetic nephropathy *via* GPR43-mediated inhibition of oxidative stress and NF-κB signaling. Oxid Med Cell Longev 2020; 2020: 4074832.
26. Qiao S, Liu R, Lv C, et al. Bergenin impedes the generation of extracellular matrix in glomerular mesangial cells and ameliorates diabetic nephropathy in mice by inhibiting oxidative stress *via* the mTOR/β-TrcP/Nrf2 pathway. Free Radic Biol Med 2019; 145: 118-35.
27. Bellezza I, Giambanco I, Minelli A, Donato R. Nrf2-Keap1 signaling in oxidative and reductive stress. Biochim Biophys Acta Mol Cell Res 2018; 1865: 721-33.
28. Zhang H, Qi S, Song Y, Ling C. Artemisinin attenuates early renal damage on diabetic nephropathy rats through suppressing TGF-β1 regulator and activating the Nrf2 signaling pathway. Life Sci 2020; 256: 117966.
29. Conti I, Varano G, Simioni C, et al. miRNAs as influencers of cell-cell communication in tumor microenvironment. Cells 2020; 9: 220.
30. Shen Y, Tong ZW, Zhou Y, et al. Inhibition of lncRNA-PAX8-AS1-N directly associated with VEGF/TGF-β1/8-OhdG enhances podocyte apoptosis in diabetic nephropathy. Eur Rev Med Pharmacol Sci 2020; 24: 6864-72.
31. Dong H, Qiang Z, Chai D, et al. Nrf2 inhibits ferroptosis and protects against acute lung injury due to intestinal ischemia reperfusion *via* regulating SLC7A11 and HO-1. Aging (Albany NY) 2020; 12: 12943-59.